mater.scichina.com link.springer.com Published online 7 July 2023 | https://doi.org/10.1007/s40843-023-2478-6

Achieving identical glassy state through different thermal paths

Jianing Wang[1,2], Lijian Song[1,2*], Yurong Gao[1], Bowen Zang[1,2], Meng Gao[1,2], Juntao Huo[1,2], Lina Hu[3] and Jun-Qiang Wang[1,2*]

ABSTRACT **The enthalpy relaxation and recovery processes of an Au-based metallic glass model were studied using high-precision nanocalorimetry. The glassy states after isothermal and isochronal annealing were compared, and it was revealed that the relaxation peaks for slightly and isochronally annealed glasses were narrower compared with slightly and isothermally annealed glasses, although they have the same enthalpy. This reveals a typical thermal history-dependent behavior. Interestingly, when the glasses were heavily annealed, the relaxation peaks of both isothermally and isochronally annealed glasses became identical, denoting no relation to thermal histories. Further relaxation kinetics studies revealed that dependence on thermal paths occurred in the β-relaxation stage, while the glassy states became identical when the α-relaxation stage was reached regardless of the thermal paths. This is attributed to the ergodic characteristic of cooperative atomic motions during the α relaxation. The difference between β and α relaxations in dependence on annealing paths is helpful for precisely controlling the glass properties.**

Keywords: glassy state, thermal paths, relaxation kinetics, α relaxation, β relaxation

INTRODUCTION

Glasses are materials with disordered atomic packing structures and nonequilibrium thermodynamic characteristics. Based on potential landscape theory, glasses comprise plenty of local structures with different energy states [1–4]. Thus, obtaining two identical glasses is difficult, although the fabrication process is generally the same. Some researchers tried to eliminate the thermal history of glass by annealing it before any tests or applications [5–9]. When annealed close to the glass transition temperature (T_g), the glass reaches the supercooled liquid state [10–12], which is in thermodynamic equilibrium but still in a metastable state. This annealing process can be considered a normalization process of the glassy state. That is, all the as-prepared glasses reach the same state after being annealed at temperatures close to T_g. This normalization method is universal for annealed samples [6,13,14]. It is interesting to determine when the memory of thermal histories is erased and whether it occurs before or at the equilibrium state.

Enthalpy relaxation has a strong influence on the physical or functional properties of glasses. For instance, the enthalpy relaxation of Fe-based metallic glasses (MGs) releases residual stress and enhances soft magnetic performance [15–18]. However, relaxing to the same energy state through different annealing paths does not yield the same properties, implying that the relaxation path is as crucial as the energy state [19–24]. It needs to be found whether the same glassy state can be achieved through different annealing paths.

There are different types of relaxation kinetics during annealing, such as α relaxation and β relaxation [2,25–27]. Generally, α relaxation depends on cooperative atomic motion, while β relaxation is related to local structural rearrangements [2,25,28–31]. In the annealing treatment, when the annealing time is long enough, β relaxation gradually merges and eventually enters the α relaxation stage. During the β-relaxation stage, the soft magnetism and hardness of glass can be considerably enhanced, and during the α-relaxation stage, soft magnetic properties change slightly, but its plasticity deteriorates [32–35]. Meanwhile, two-step annealing activates the Kovacs memory effect [36], which can improve the mechanical and magnetic properties of MGs in comparison with single-step annealing treatment [37,38]. Several studies have suggested that the coupling of different relaxation kinetics or relaxation paths plays a key role in glassy state evolution [39–43]. However, these studies did not state how to obtain the identical normalized glassy state through different annealing paths, and the underlying physical mechanism is still unclear.

In this work, the enthalpy evolution of a model MG ($Au_{49}Cu_{26.9}Ag_{5.5}Pd_{2.3}Si_{16.3}$, at%) [10,44–47] upon continuous cooling and isothermal annealing was studied using high-precision flash differential scanning calorimetry (DSC). The enthalpy value and shape of the relaxation peak were used to characterize the glassy state. Enthalpy represents the energy level of glass, which is a crucial parameter, and the relaxation peak shape with the same area (i.e., enthalpy value) represents the distribution of energy states, which can reflect the influence of annealing paths. The underlying mechanisms were studied and discussed.

EXPERIMENTAL SECTION

Sample preparation

Ingot with a nominal composition of $Au_{49}Cu_{26.9}Ag_{5.5}Pd_{2.3}Si_{16.3}$

[1] CAS Key Laboratory of Magnetic Materials and Devices, and Zhejiang Province Key Laboratory of Magnetic Materials and Application Technology, Ningbo Institute of Materials Technology and Engineering, Chinese Academy of Sciences, Ningbo 315201, China
[2] Center of Materials Science and Optoelectronics Engineering, University of Chinese Academy of Sciences, Beijing 100049, China
[3] Key Laboratory for Liquid-Solid Structural Evolution and Processing of Materials, Ministry of Education, Shandong University, Jinan 250061, China
* Corresponding authors (emails: jqwang@nimte.ac.cn (Wang JQ); songlj@nimte.ac.cn (Song L))

(at%) was prepared through the arc melting of high-purity constituent elements in a Ti-gettered high-purity argon atmosphere. The ingot was flipped and remelted five times to obtain a homogeneous master alloy. MG ribbons were prepared using a single roller melt spinner operated under a circumferential speed of 40 m s^{-1}.

Flash DSC measurements

Nanocalorimetry experiments were performed using a Mettler Toledo Flash DSC 1 with a mechanical pump refrigeration system and nitrogen purge. A sample with dimensions of about 50 μm × 50 μm × 20 μm was cut from an MG ribbon and then loaded onto the center of the chip sensor under an optical microscope. All experimental data in this paper were acquired from the same sample. The mass of the Flash DSC sample was estimated from the melting enthalpy. The melting enthalpy of the Flash DSC sample used in this study was about 19.45 μJ. The specific melting enthalpy of the melt-spun Au-based MG is 40.2 J g^{-1} [10,45]. Thus, the mass of the Flash DSC sample was determined to be $19.45 \times 10^{-6}/40.2$ g ≈ 484 ng (3.82×10^{-9} mol). To examine the relaxation paths, the sample was isothermally annealed at 373, 379, 385, 391, and 397 K for various annealing times (t_a) and/or cooled from the initial temperature of continuous cooling (T_s = 403 K) to annealing temperature (T_a) at cooling rates of ϕ = 1, 2, 3, 5, 10, 20, 30, 50, and 100 K s^{-1}, where all T_s and T_a were below T_g. The identical relaxation enthalpy of the sample during cooling and isothermal annealing was determined by the evolution of the enthalpy change with the cooling rate or annealing time. Four representative heating rates (R_h = 100, 200, 500, and 1000 K s^{-1}) were used to estimate the activation energy of the relaxation processes.

RESULTS

Relaxation of the sample under two different annealing paths

In Fig. 1a, the sample underwent two different annealing paths, namely, continuous cooling (①) and isothermal annealing (②), to reach the same enthalpy state at temperature T_a, and the thermal protocols are shown in Fig. 1b. In the continuous cooling process, the sample was cooled from the melt at 693 K (liquidus temperature: T_L = 645 K) to T_s = 403 K at a cooling rate R_c = 6000 K s^{-1}, which is larger than the critical cooling rate

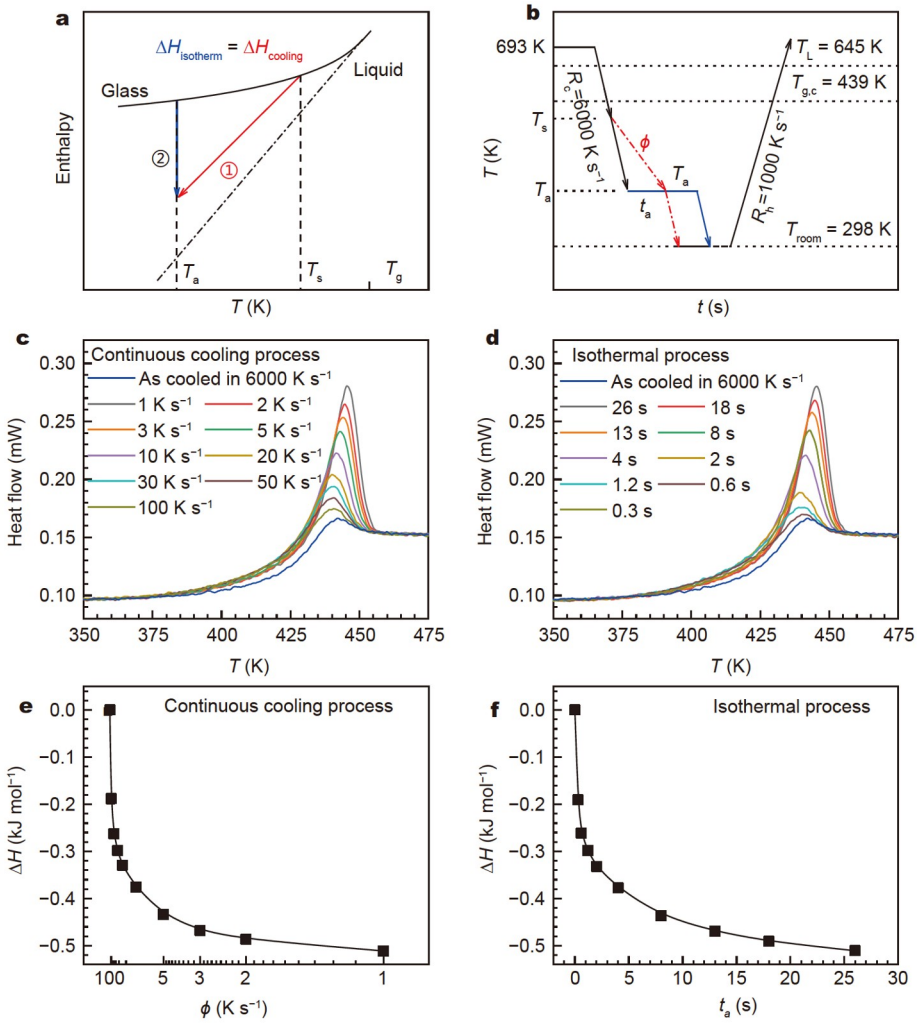

Figure 1 (a) Schematic of continuous cooling and isothermal annealing paths in the enthalpy-temperature phase diagram. (b) Thermal protocols for continuous cooling and isothermal annealing. (c) Flash DSC traces near the T_g for the samples cooled from 403 to 385 K at different rates. (d) Flash DSC traces of the sample relaxed at 385 K for various annealing times (t_a). (e) Relaxation enthalpy changes with the cooling rate (ϕ). (f) Relaxation enthalpy changes with annealing time t_a at T_a = 385 K.

(~1600 K s^{-1}), to obtain a fully glassy state [10,48,49]. The sample was then cooled from T_s to T_a at cooling rates of ϕ = 1, 2, 3, 5, 10, 20, 30, 50, and 100 K s^{-1}. For the isothermal annealing process, the sample was cooled from 693 K to T_a at a cooling rate of R_c = 6000 K s^{-1}, and then t_a was gradually increased until the relaxation enthalpy of the isothermal process was equal to that of the continuous cooling process. Finally, the recovery process and glass transition behavior for the relaxed glasses were measured using Flash DSC at a heating rate of R_h = 1000 K s^{-1}. The relaxation peak during the recovery process was obtained by subtracting the Flash DSC trace of the as-cooled glass from that of the relaxed glasses, and the relaxation enthalpy was obtained by integrating the corresponding relaxation peak.

Fig. 1c, d show the Flash DSC traces for the samples relaxed upon continuous cooling from T_s = 403 K to T_a = 385 K and relaxed upon isothermal annealing at T_a = 385 K, respectively. The height of the endothermic overshoots and the peak temperature increases as the cooling rate decreases or the isothermal annealing time increases. Thus, it was revealed that continuous cooling and isothermal annealing have similar influences on relaxation behavior and enthalpy state. Fig. 1e, f illustrate the change in enthalpy *versus* the cooling rate (ϕ) of the continuous cooling process and the annealing time of the isothermal annealing process, respectively. The relaxation enthalpy (ΔH) decreases monotonically with decreasing cooling rate and increasing annealing time.

Comparison of the relaxation peaks in two annealing paths

As shown in Fig. 1a, the same enthalpy state can be reached by continuous cooling and isothermal annealing, but the same relaxation enthalpy does not represent the identical glassy state. If we compare the relaxation peaks, the glasses relaxed to the same enthalpy state through different thermal paths showing distinct shapes, as shown in Fig. 2a. The comparison of heat flows of the glasses cooled to 385 K at six representative rates, ϕ = 100, 50, 30, 10, 5, and 1 K s^{-1}, corresponding to the annealing times, t_a = 0.3, 0.6, 1.2, 4, 8, and 26 s, is given in Fig. 2a–f. For the fast-cooling rates, $\phi \geqslant$ 30 K s^{-1}, the relaxation peak of the continuously cooled samples is narrower and shows a higher peak temperature than that of the isothermally annealed samples, reflecting that the glassy states obtained by continuous cooling and isothermal annealing are not identical. With decreasing cooling rate and increasing isothermal annealing time, the relaxation peaks become gradually identical, reflecting that the influence of thermal histories disappears when the sample reaches deep-relaxed states. This indicates that the dependence of glassy states on annealing paths is different in different energy states.

To analyze the dependence of glassy states on annealing paths systematically, the full width at half maximum (FWHM) of relaxation peaks was introduced and used along with the enthalpy value to characterize the relaxation peak shapes. FWHM is a key parameter reflecting the distribution of energy states in the glass. Generally, a small FWHM of the relaxation peak means a more homogeneous structure of glass [50,51]. Fig. 3a exhibits the definition of the FWHM and the relaxation enthalpy of a relaxation peak. For all continuous cooling and isothermal annealing processes, the FWHM decreases monotonically with increasing relaxation enthalpy, as shown in Fig. 3b–f. For slightly annealed glasses with the same relaxation enthalpy, the continuously cooled sample has a relaxation peak with a smaller FWHM than the isothermally annealed sample. Along with decreasing enthalpy, the FWHM values of the relaxation peaks from the samples with different thermal paths become identical.

Activation energy of relaxations

The underlying mechanisms behind the differences of relaxation

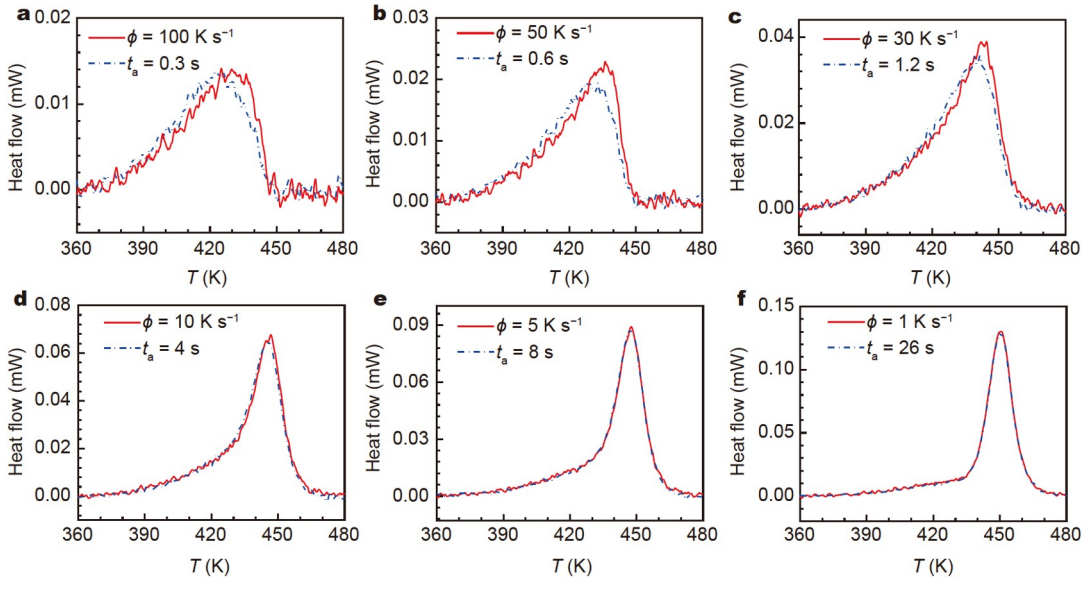

Figure 2 (a) Heat flow peaks of the sample isothermally annealed at T_a = 385 K for t_a = 0.3 s (blue) and cooled from 403 to 385 K at ϕ = 100 K s^{-1} (red). (b) Heat flow peaks of the sample isothermally annealed at T_a = 385 K for t_a = 0.6 s (blue) and cooled from 403 to 385 K at ϕ = 50 K s^{-1} (red). (c) Heat flow peaks of the sample isothermally annealed at T_a = 385 K for t_a = 1.2 s (blue) and cooled from 403 to 385 K at ϕ = 30 K s^{-1} (red). (d) Heat flow peaks of the sample isothermally annealed at T_a = 385 K for t_a = 4 s (blue) and cooled from 403 to 385 K at ϕ = 10 K s^{-1} (red). (e) Heat flow peaks of the sample isothermally annealed at T_a = 385 K for t_a = 8 s (blue) and cooled from 403 to 385 K at ϕ = 5 K s^{-1} (red). (f) Heat flow peaks of the sample isothermally annealed at T_a = 385 K for t_a = 26 s (blue) and cooled from 403 to 385 K at ϕ = 1 K s^{-1} (red).

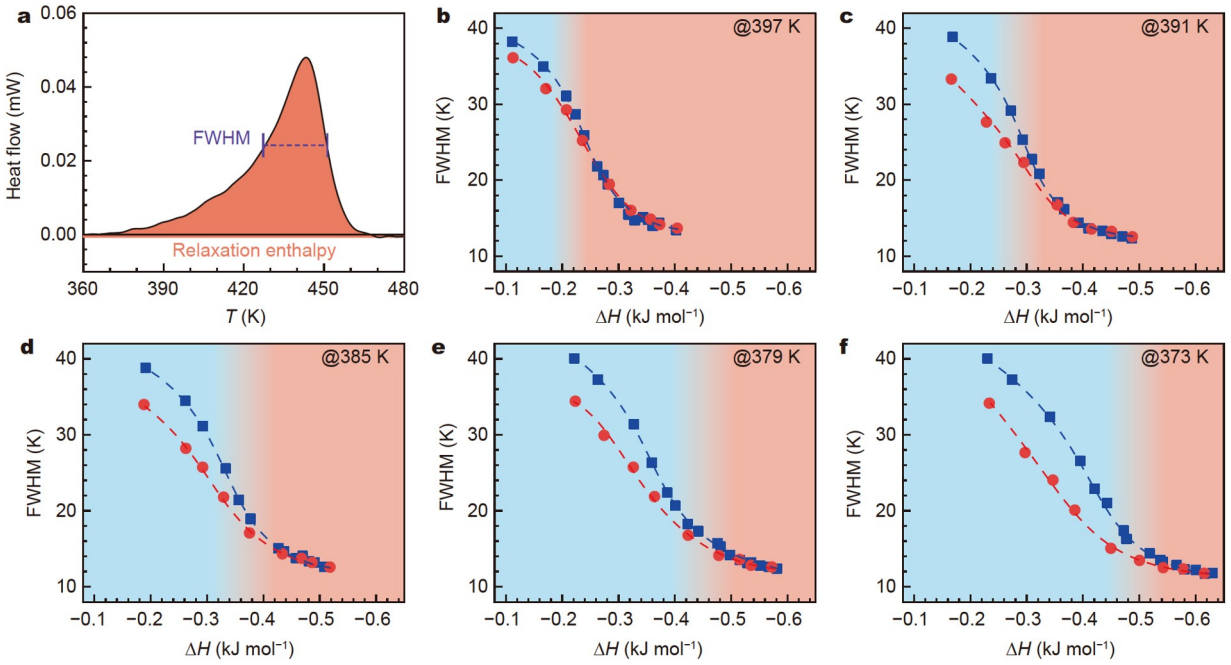

Figure 3 (a) FWHM and the area of the relaxation peak (relaxation enthalpy, ΔH) are used to represent the glassy state. (b–f) Evolution of FWHM with ΔH of isothermal and continuous cooling annealed samples. The red solid circle represents the sample annealed by the continuous cooling process, and the blue square represents the sample annealed by the isothermal process. The dashed lines are plotted as a guide. The background color illustrates the transition from distinct glassy (blue) to identical glassy states (red) through two annealing paths.

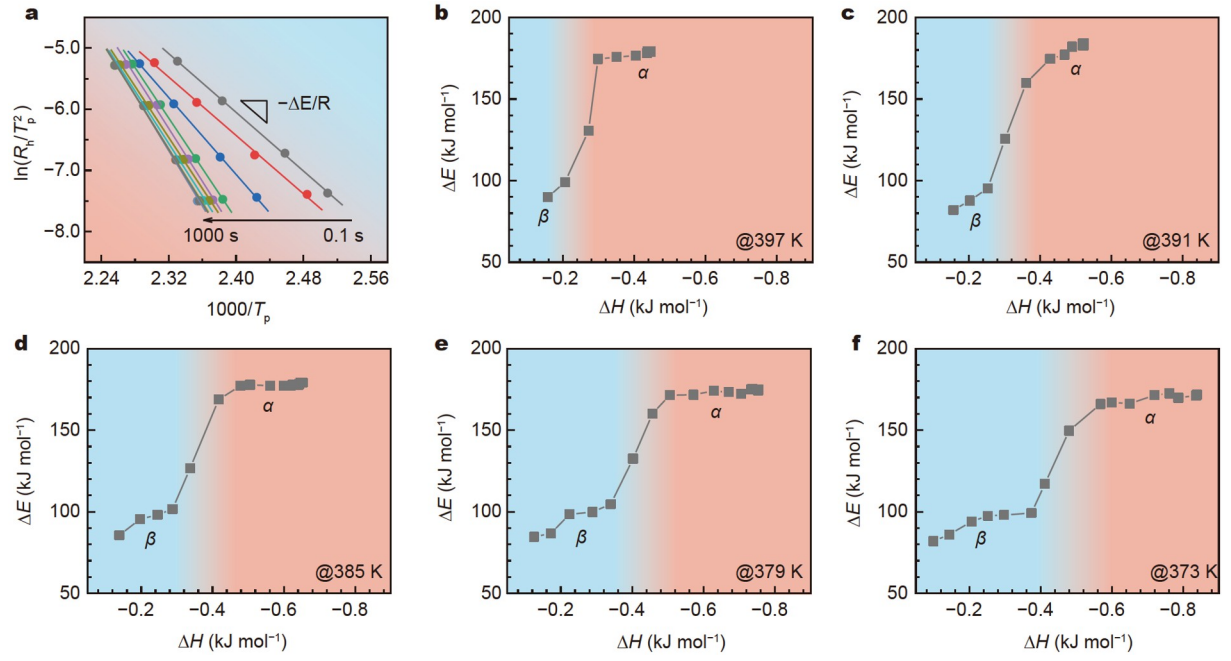

Figure 4 (a) Kissinger plots of the relaxation peak temperatures (T_p) for samples annealed at T_a = 397 K for different annealing times t_a = 0.1–1000 s. The relaxation activation energy (ΔE) is determined by the slope. (b–f) Activation energy (ΔE) *versus* relaxation enthalpy (ΔH). The background color is adopted from Fig. 3 to illustrate the transition from distinct glassy (blue) to identical glassy states (red) through two annealing paths.

peaks were investigated by studying the relaxation kinetics of different relaxed glasses using the Kissinger method $([\partial \ln(\phi/T_p^2)]/[\partial(1/T_p)]=-\Delta E/R$, where R and ΔE are the gas constant and activation energy, respectively). Fig. 4a shows the heating rate dependence of relaxation peak temperatures for samples annealed at T_a = 397 K for various times (t_a). Linear fitting by the Kissinger plot gives the activation energy of the relaxed glass. The relaxation activation energy increases from 80–100 to ~170 kJ mol^{-1} with decreasing relaxation enthalpy. At the initial relaxation stage, ΔE is consistent with the activation energy of β relaxation, that is, $\Delta E_\beta \approx 26RT_g$ (T_g = 401 K at 20 K min^{-1}). For deep-relaxed samples, the estimated ΔE coincides with that of α relaxation, as shown in Fig. 4b–f [9,44,52,53]. It is interesting to note that, compared with the data from Fig. 3,

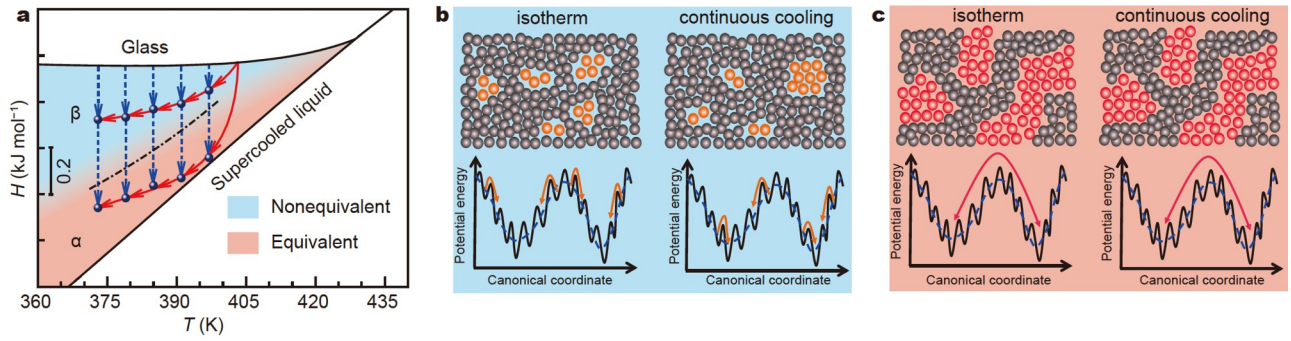

Figure 5 (a) Schematic map of enthalpy changes during glass annealing. The black dash-dotted line indicates the boundary between equivalent and nonequivalent peaks. (b, c) Evolution of atomic motions and the corresponding energy landscape. Each corresponding energy landscape is located below its atomic motions. The orange atoms represent the local β relaxation region, while the red atoms represent the collective α relaxation region.

the glassy states yielded by different annealing paths merged when the relaxation kinetics turned into the α relaxation stage. Moreover, it should be noted that the relaxation modes defined by Flash DSC are consistent with that measured by dynamic mechanical analysis (see Fig. S1) and in previous studies [46,54,55].

DISCUSSION

To understand the underlying mechanism for the thermal history-dependent behavior, the above difference between β relaxation and α relaxation is illustrated in an enthalpy-temperature diagram. Fig. 5a illustrates the trajectories for the continuous cooling and isothermal annealing paths. The blue-shaded area, which corresponds to the β relaxation region, represents the glassy state that is sensitive to annealing paths. The red-shaded area, which corresponds to the α relaxation region, represents the glassy states that are independent of annealing paths. For instance, when the sample is cooled from 403 K to T_a = 397, 391, 385, 379, and 373 K at a high cooling rate of ϕ = 100 K s^{-1}, the enthalpy relaxation kinetics remains in β relaxation, and the relaxation peaks are distinct from those from the isothermally annealed samples. In contrast, when the sample is cooled slowly at 1 K s^{-1}, the enthalpy relaxation kinetics is in α relaxation, and the relaxation peaks are identical to those from the isothermally annealed samples. Thus, it is revealed that the glassy states in the β-relaxation region are dependent on thermal histories, while the glassy states in the α-relaxation region are independent of thermal histories. In the energy landscape view, this should be related to ergodicity during the energy evolution. The collective α relaxation travels over a big barrier that is ergodic to erase its historical state [10,56–60], while the local β relaxation can only overcome a small barrier that is nonergodic and dependent on thermal histories. In terms of the energy landscape, the continuous cooling process triggers different local structures from high to low temperatures due to temperature-dependent atomic motions [61]. The larger activation energy at higher temperatures triggers collective atomic motions and leads to a narrower FWHM, denoting a more homogenous structure, as illustrated in Fig. 5b. However, the α relaxation with the percolation of atomic motions activates ergodic motions, as shown in Fig. 5c. Furthermore, the same test was applied to $(La_{0.5}Ce_{0.5})_{65}Al_{10}Cu_{25}$ MG (see Fig. S2) and was observed to be highly consistent with that of the Au-based MG.

The far-from-equilibrium nature of glasses provides a chance to modulate their properties by changing their enthalpy state. Intriguingly, this work demonstrates that although the enthalpy state of glasses is the same, the distribution of microstates may vary due to different thermal histories, particularly for the lightly relaxed glasses. The FWHM is related to microstate distribution. It is expected that the relaxation peaks in heat flows provide a simple and reasonable signal to understand relaxation behaviors not only from thermodynamic and kinetic viewpoints but also from structural information.

CONCLUSIONS

The relaxation behaviors of MGs during continuous cooling and isothermal annealing were studied systemically in the enthalpy space. Glasses in the β-relaxation stage have a thermal history memory characterized by nonequivalent heat flow peaks, while α relaxation stage has an identical glassy state that is independent of thermal paths. The findings extend heat flow to the structural evolution of glassy states and enrich the meaning of relaxation peaks besides the thermodynamic and kinetic information. These results could facilitate the precise control of glass properties and the design of advanced properties.

Received 24 February 2023; accepted 19 April 2023; published online 7 July 2023

1 Charbonneau P, Kurchan J, Parisi G, *et al.* Fractal free energy landscapes in structural glasses. Nat Commun, 2014, 5: 3725
2 Debenedetti PG, Stillinger FH. Supercooled liquids and the glass transition. Nature, 2001, 410: 259–267
3 Rodney D, Schuh CA. Yield stress in metallic glasses: The jamming-unjamming transition studied through Monte Carlo simulations based on the activation-relaxation technique. Phys Rev B, 2009, 80: 184203
4 Kahl A, Koeppe T, Bedorf D, *et al.* Dynamical and quasistatic structural relaxation paths in $Pd_{40}Ni_{40}P_{20}$ glass. Appl Phys Lett, 2009, 95: 201903
5 Hu L, Zhou C, Zhang C, *et al.* Thermodynamic anomaly of the sub-T_g relaxation in hyperquenched metallic glasses. J Chem Phys, 2013, 138: 174508
6 Luo P, Li YZ, Bai HY, *et al.* Memory effect manifested by a Boson peak in metallic glass. Phys Rev Lett, 2016, 116: 175901
7 Launey ME, Kruzic JJ, Li C, *et al.* Quantification of free volume differences in a $Zr_{44}Ti_{11}Ni_{10}Cu_{10}Be_{25}$ bulk amorphous alloy. Appl Phys Lett, 2007, 91: 051913
8 Yue Y. Revealing the nature of glass by the hyperquenching-annealing-calorimetry approach. J Non-Crystalline Solids-X, 2022, 14: 100099
9 Zhou C, Yue Y, Hu L. Revealing the connection between the slow β relaxation and sub-T_g enthalpy relaxation in metallic glasses. J Appl Phys, 2016, 120: 225110
10 Wang JQ, Shen Y, Perepezko JH, *et al.* Increasing the kinetic stability of bulk metallic glasses. Acta Mater, 2016, 104: 25–32

11 Cangialosi D, Boucher VM, Alegría A, *et al.* Direct evidence of two equilibration mechanisms in glassy polymers. Phys Rev Lett, 2013, 111: 095701
12 Liu S, Yu Y, Liu L, *et al.* Hierarchical aging pathways and signatures of thermodynamic transition in molecular glasses. Sci China Mater, 2019, 62: 864–872
13 Aji DPB, Wen P, Johari GP. Memory effect in enthalpy relaxation of two metal-alloy glasses. J Non-Crystalline Solids, 2007, 353: 3796–3811
14 Gallino I, Cangialosi D, Evenson Z, *et al.* Hierarchical aging pathways and reversible fragile-to-strong transition upon annealing of a metallic glass former. Acta Mater, 2018, 144: 400–410
15 Inoue A, Kong FL, Han Y, *et al.* Development and application of Fe-based soft magnetic bulk metallic glassy inductors. J Alloys Compd, 2018, 731: 1303–1309
16 Luo Q, Li D, Cai M, *et al.* Excellent magnetic softness-magnetization synergy and suppressed defect activation in soft magnetic amorphous alloys by magnetic field annealing. J Mater Sci Tech, 2022, 116: 72–82
17 Liu G, Xiao Z, Wang N, *et al.* Synthesis and characterization of soft-magnetic $(Fe_{0.7}Co_{0.3})_{75}B_{21}Ta_4$ metallic glasses by annealing and cryogenic treatment. J Non-Crystalline Solids, 2022, 581: 121411
18 Naohara T. Aging effects of the microstructure and soft magnetic properties in an amorphous Fe–Si–B–Nb alloy. Appl Phys Lett, 1996, 68: 1012–1014
19 Ketov SV, Sun YH, Nachum S, *et al.* Rejuvenation of metallic glasses by non-affine thermal strain. Nature, 2015, 524: 200–203
20 Tang Y, Xiao HB, Wang XD, *et al.* Mechanical property and structural changes by thermal cycling in phase-separated metallic glasses. J Mater Sci Tech, 2021, 78: 144–154
21 Ri MC, Ding DW, Sun YH, *et al.* Microstructure change in Fe-based metallic glass and nanocrystalline alloy induced by liquid nitrogen treatment. J Mater Sci Tech, 2021, 69: 1–6
22 Guo W, Yamada R, Saida J, *et al.* Various rejuvenation behaviors of Zr-based metallic glass by cryogenic cycling treatment with different casting temperatures. Nanoscale Res Lett, 2018, 13: 398
23 Saida J, Yamada R, Wakeda M, *et al.* Thermal rejuvenation in metallic glasses. Sci Tech Adv Mater, 2017, 18: 152–162
24 Rajpoot D, Narayan RL, Zhang L, *et al.* Fracture toughness of a rejuvenated β-Ti reinforced bulk metallic glass matrix composite. J Mater Sci Tech, 2022, 106: 225–235
25 Yu HB, Wang WH, Bai HY, *et al.* The β-relaxation in metallic glasses. Natl Sci Rev, 2014, 1: 429–461
26 Roland CM, Schroeder MJ, Fontanella JJ, *et al.* Evolution of the dynamics in 1,4-polyisoprene from a nearly constant loss to a Johari-Goldstein β-relaxation to the α-relaxation. Macromolecules, 2004, 37: 2630–2635
27 Ngai KL, Shahin Thayyil M, Wang LM. Quasielastic neutron scattering evidence of coupling of caged molecule dynamics to JG β-relaxation. J Mol Liquids, 2017, 247: 300–303
28 Wang Q, Zhang ST, Yang Y, *et al.* Unusual fast secondary relaxation in metallic glass. Nat Commun, 2015, 6: 7876
29 Fujima T, Frusawa H, Ito K. Merging of α and slow β relaxation in supercooled liquids. Phys Rev E, 2002, 66: 031503
30 Zhao LZ, Xue RJ, Zhu ZG, *et al.* A fast dynamic mode in rare earth based glasses. J Chem Phys, 2016, 144: 204507
31 Evenson Z, Koschine T, Wei S, *et al.* The effect of low-temperature structural relaxation on free volume and chemical short-range ordering in a $Au_{49}Cu_{26.9}Si_{16.3}Ag_{5.5}Pd_{2.3}$ bulk metallic glass. Scripta Mater, 2015, 103: 14–17
32 He N, Song L, Xu W, *et al.* The evolution of relaxation modes during isothermal annealing and its influence on properties of Fe-based metallic glass. J Non-Crystalline Solids, 2019, 509: 95–98
33 Chen S, Li S, Ma J, *et al.* Ultrasonic vibration accelerated aging in La-based bulk metallic glasses. J Non-Crystalline Solids, 2020, 535: 119967
34 Schuh CA, Hufnagel TC, Ramamurty U. Mechanical behavior of amorphous alloys. Acta Mater, 2007, 55: 4067–4109
35 Zhang LT, Duan YJ, Crespo D, *et al.* Dynamic mechanical relaxation and thermal creep of high-entropy $La_{30}Ce_{30}Ni_{10}Al_{20}Co_{10}$ bulk metallic glass. Sci China-Phys Mech Astron, 2021, 64: 296111
36 Kovacs AJ. Transition vitreuse dans les polymères amorphes. Etude phénoménologique. Fortschr Hochpolym Forsch, 1963, 3: 394–507
37 Ohta M, Hasegawa R. Soft magnetic properties of magnetic cores assembled with a high B_s Fe-based nanocrystalline alloy. IEEE Trans Magn, 2017, 53: 1–5
38 Xia GT, Wang YG, Dai J, *et al.* Effects of Cu cluster evolution on soft magnetic properties of $Fe_{83}B_{10}C_6Cu_1$ metallic glass in two-step annealing. J Alloys Compd, 2017, 690: 281–286
39 Song L, Xu W, Huo J, *et al.* Activation entropy as a key factor controlling the memory effect in glasses. Phys Rev Lett, 2020, 125: 135501
40 Hem J, Crauste-Thibierge C, Clément F, *et al.* Simultaneous memory effects in the stress and in the dielectric susceptibility of a stretched polymer glass. Phys Rev E, 2021, 103: L040502
41 Koike A, Tomozawa M. Towards the origin of the memory effect in oxide glasses. J Non-Crystalline Solids, 2008, 354: 3246–3253
42 Di X, Win KZ, McKenna GB, *et al.* Signatures of structural recovery in colloidal glasses. Phys Rev Lett, 2011, 106: 095701
43 Lei Y, Cummins K, Lacks DJ. First-principles enthalpy landscape analysis of structural recovery in glasses. J Polym Sci B Polym Phys, 2010, 41: 2302–2306
44 Song L, Xu W, Huo J, *et al.* Two-step relaxations in metallic glasses during isothermal annealing. Intermetallics, 2018, 93: 101–105
45 Pogatscher S, Uggowitzer PJ, Löffler JF. *In-situ* probing of metallic glass formation and crystallization upon heating and cooling *via* fast differential scanning calorimetry. Appl Phys Lett, 2014, 104: 251908
46 Evenson Z, Naleway SE, Wei S, *et al.* β relaxation and low-temperature aging in a Au-based bulk metallic glass: From elastic properties to atomic-scale structure. Phys Rev B, 2014, 89: 174204
47 Monnier X, Cangialosi D, Ruta B, *et al.* Vitrification decoupling from α-relaxation in a metallic glass. Sci Adv, 2020, 6: 1454
48 Schawe JEK, Löffler JF. Kinetics of structure formation in the vicinity of the glass transition. Acta Mater, 2022, 226: 117630
49 Schawe JEK, Löffler JF. Existence of multiple critical cooling rates which generate different types of monolithic metallic glass. Nat Commun, 2019, 10: 1337
50 Qiao JC, Wang Q, Crespo D, *et al.* Amorphous physics and materials: Secondary relaxation and dynamic heterogeneity in metallic glasses: A brief review. Chin Phys B, 2017, 26: 016402
51 Jiao W, Wen P, Peng HL, *et al.* Evolution of structural and dynamic heterogeneities and activation energy distribution of deformation units in metallic glass. Appl Phys Lett, 2013, 102: 101903
52 Chen HS. On mechanisms of structural relaxation in a $Pd_{48}Ni_{32}P_{20}$ glass. J Non-Crystalline Solids, 1981, 46: 289–305
53 Luo P, Wen P, Bai HY, *et al.* Relaxation decoupling in metallic glasses at low temperatures. Phys Rev Lett, 2017, 118: 225901
54 Yang Q, Peng SX, Wang Z, *et al.* Shadow glass transition as a thermodynamic signature of β relaxation in hyper-quenched metallic glasses. Natl Sci Rev, 2020, 7: 1896–1905
55 Pelletier JM, Cardinal S, Qiao JC, *et al.* Main and secondary relaxations in an Au-based bulk metallic glass investigated by mechanical spectroscopy. J Alloys Compd, 2016, 684: 530–536
56 Ruta B, Pineda E, Evenson Z. Relaxation processes and physical aging in metallic glasses. J Phys-Condens Matter, 2017, 29: 503002
57 Soriano D, Zhou H, Hilke S, *et al.* Relaxation dynamics of Pd–Ni–P metallic glass: Decoupling of anelastic and viscous processes. J Phys-Condens Matter, 2021, 33: 164004
58 Liu C, Pineda E, Crespo D, *et al.* Sub-T_g relaxation times of the α process in metallic glasses. J Non-Crystalline Solids, 2017, 471: 322–327
59 Aji DPB, Johari GP. Enthalpy and entropy changes on structural relaxation of $Mg_{65}Cu_{25}Tb_{10}$ glass. ThermoChim Acta, 2010, 503-504: 121–131
60 Mei JN, Soubeyroux JL, Blandin JJ, *et al.* Structural relaxation of $Ti_{40}Zr_{25}Ni_8Cu_9Be_{18}$ bulk metallic glass. J Non-Crystalline Solids, 2011, 357: 110–115
61 Wang YJ, Du JP, Shinzato S, *et al.* A free energy landscape perspective on the nature of collective diffusion in amorphous solids. Acta Mater, 2018, 157: 165–173

Acknowledgements This work was supported by the National Key R&D Program of China (2018YFA0703600), the National Natural Science Foun-

dation of China (51922102, 52001319, 52271158, 92163108, and 52231006), Zhejiang Provincial Natural Science Foundation (LGF22E010002, LZ22A030001, and LR22E010004), the "Pioneer and Leading Goose" R&D Program of Zhejiang (2022C01023), and Ningbo Key Scientific and Technological Project (2019B10051).

Author contributions Wang J performed the experiments with the assistance of Gao Y and Zang B. Wang J, Song L, Gao M, Huo J, Hu L and Wang JQ performed the data analysis. Wang J, Song L, and Wang JQ wrote the paper with input from all authors. Song L and Wang JQ supervised the work. All authors discussed the results.

Conflict of interest The authors declare that they have no conflict of interest.

Supplementary information Supporting data are available in the online version of the paper.

Jianing Wang received his BSc degree in materials science and engineering from Qinghai University in 2020. He is currently a PhD candidate in materials physics and chemistry under the supervision of Prof. Jun-Qiang Wang at Ningbo Institute of Materials Technology and Engineering, Chinese Academy of Sciences. His PhD research focuses on the relaxation dynamics of metallic glasses.

Lijian Song received his PhD degree in materials physics and chemistry in 2018 under the supervision of Prof. Jun-Qiang Wang at Ningbo Institute of Materials Technology and Engineering, Chinese Academy of Sciences. He is currently an associate professor at Ningbo Institute of Materials Technology and Engineering, Chinese Academy of Sciences. His research focuses on the relaxation kinetics and crystallization behaviors of metallic glasses.

Jun-Qiang Wang received his PhD degree from the Institute of Physics, Chinese Academy of Sciences in 2010. Then he worked as a postdoctoral fellow at Tohoku University (Japan) and the University of Wisconsin-Madison (USA) from 2010 to 2014. Now he is a professor at Ningbo Institute of Materials Technology and Engineering, Chinese Academy of Sciences. His research interests include the non-equilibrium thermodynamics and functional properties of glassy materials.

通过不同退火路径获得相同的玻璃态

王家宁[1,2], 宋丽建[1,2*], 高玉蓉[1], 臧博闻[1,2], 高萌[1,2], 霍军涛[1,2], 胡丽娜[3], 王军强[1,2*]

摘要 本文以金基金属玻璃为模型，使用高精度闪速差示扫描量热法研究了等温退火和连续降温退火对焓弛豫和回复过程的影响. 发现即使玻璃的能量(焓)一样，两种退火路径获得的玻璃的状态也可能不同. 对于短时间等温退火或快速连续降温退火得到的高能量玻璃，两种退火路径获得的玻璃状态明显不同: 连续降温退火得到的玻璃的弛豫峰更窄，而等温退火得到的玻璃弛豫峰更宽. 但是，对于长时间等温退火或慢速连续降温退火得到的低能量玻璃，两种退火路径获得的玻璃状态趋于相同，即弛豫峰完全重合. 弛豫动力学结果表明，高能量玻璃处在β弛豫阶段，具有热历史依赖性. 而低能量玻璃处在α弛豫阶段，玻璃状态与热历史无关，这主要是因为α弛豫具有较强的协同性，具有各态遍历特征，使结构均一化. 这些发现对精准调控玻璃性质具有重要意义.